NASA Technical Memorandum 4760
ARL Technical Report 1389

Rotating Shake Test and Modal Analysis of a Model Helicopter Rotor Blade

W. Keats Wilkie, Paul H. Mirick, and Chester W. Langston
Vehicle Technology Center
U.S. Army Research Laboratory
Langley Research Center • Hampton, Virginia

National Aeronautics and Space Administration
Langley Research Center • Hampton, Virginia 23681-0001

June 1997

Available electronically at the following URL address: http://techreports.larc.nasa.gov/ltrs/ltrs.html

Printed copies available from the following:

NASA Center for AeroSpace Information
800 Elkridge Landing Road
Linthicum Heights, MD 21090-2934
(301) 621-0390

National Technical Information Service (NTIS)
5285 Port Royal Road
Springfield, VA 22161-2171
(703) 487-4650

Summary

Rotating blade frequencies for a model generic helicopter rotor blade mounted on an articulated hub were experimentally determined. Tests were conducted using the Aeroelastic Rotor Experimental System (ARES) testbed in the Helicopter Hover Facility (HHF) at Langley Research Center. The measured data were compared with pretest analytical predictions of the rotating blade frequencies made using the MSC/NASTRAN finite-element computer code. The MSC/NASTRAN solution sequences used to analyze the model were modified to account for differential stiffening effects caused by the centrifugal force acting on the blade and rotating system dynamic effects. The correlation of the MSC/NASTRAN-derived frequencies with the experimental data is, in general, very good although discrepancies in the blade torsional frequency trends and magnitudes were observed. The procedures necessary to perform a rotating system modal analysis of a helicopter rotor blade with MSC/NASTRAN are outlined, and complete sample data deck listings are provided.

Introduction

Calculation of the rotating system modal properties of rotor blade and hub assemblies, particularly in the case of bearingless hub designs, often requires the use of modern finite-element computer codes. One widely used finite-element code is the commercially available MSC/NASTRAN program (refs. 1–4). Although a rotating system modal analysis can be performed using the standard release versions of MSC/NASTRAN, some potentially significant dynamic effects caused by rotation will not be accounted for properly. By modifying the standard MSC/NASTRAN solution sequence to include the additional rotational effects, a more accurate modal analysis of a rotating structure may be performed. This report documents an experimental evaluation of the ability of this modified MSC/NASTRAN procedure to accurately predict the rotating blade frequencies of a model articulated helicopter rotor blade.

Experimental Apparatus and Procedures

Test Facility

Tests were conducted in the Langley Helicopter Hover Facility (HHF) shown in figure 1. The HHF, a high-bay facility enclosed by a 30-ft by 30-ft by 20-ft coarse-mesh screen, is used for hover testing and rotorcraft model buildup and checkout prior to testing in the Langley Transonic Dynamics Tunnel (TDT). Models are mounted on the test stand such that the rotor plane of

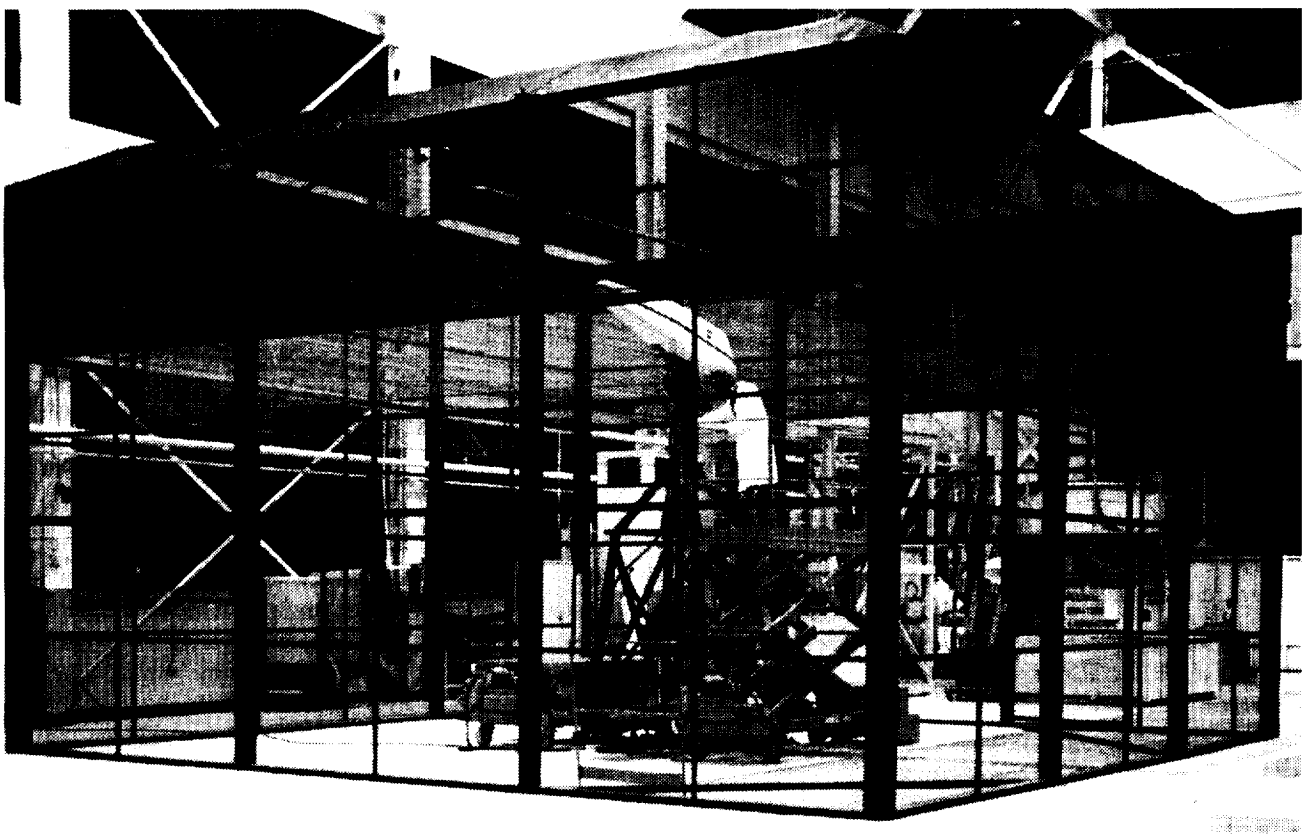

L-78-5962

Figure 1. Helicopter Hover Facility (HHF).

Table 1. Properties of Model Rotor Blade

(a) Structural properties

Inboard section radius, in.	Section spar area, in^2	Chordwise area moment of inertia, in^4	Flapwise area moment of inertia, in^4	Torsional area moment of inertia, in^4	Section mass, lb/in.	Section mass moment of inertia, $in\text{-}lb^2/in.$	Center of mass offset forward of elastic axis, in.
3.00	5.50	0.5000	0.5000	0.2632	0.4251	0.2200	0.0
6.87	0.371	0.1500	0.0500	0.1316	0.1938	0.04826	0.0
8.87	0.371	0.0250	0.0040	0.0105	0.04086	0.02505	0.0
10.625	0.371	0.0250	0.0040	0.0105	0.15113	0.05671	0.0
12.50	0.377	0.0355	0.00394	0.0394	0.14048	0.05559	0.0
13.00	0.386	0.0252	0.00249	0.00976	0.03134	0.02779	0.0
15.375	0.339	0.0252	0.00249	0.00976	0.04376	0.02961	0.0
17.85	0.278	0.03040	0.00231	0.00674	0.04123	0.02888	0.0
23.75	0.249	0.02636	0.00181	0.00565	0.0400	0.02810	0.0
28.25	0.224	0.02447	0.00151	0.00485	0.03903	0.02756	0.0
51.00	0.247	0.02447	0.00151	0.00485	0.03903	0.02756	0.0
52.75	0.279	0.02448	0.00160	0.00502	0.04125	0.02826	0.0
53.00	0.305	0.0500	0.00500	0.01435	0.07867	0.03984	–0.106
54.00	0.099	0.0400	0.00400	0.01148	0.0607	0.03563	–0.170
54.25	0.05	0.0050	0.00050	0.01435	0.01101	0.004401	–0.940

(b) Assumed material properties

Modulus of elasticity, lb/in^2	Poisson's ratio
1.0×10^7	0.3

rotation is effectively out of ground effect (15 ft, or approximately 1.6 times the rotor diameter). All hover testing in the HHF is conducted at sea level atmospheric conditions.

Model Description

A four-bladed articulated rotor hub, with coincident lead-lag and flapping hinges, was used in this experiment. The structural and inertial properties of the model blades are listed in table 1. The blades were rectangular in planform and possessed no built-in twist. A standard NACA 0012 airfoil contour was used over the aerodynamic portions of the blade. One blade was instrumented with flapwise, chordwise, and torsional-direction strain gauges mounted at three radial locations. The blade planform geometry, with strain-gauge locations indicated, is illustrated in figure 2.

The testbed for this experiment was the NASA/U.S. Army Aeroelastic Rotor Experimental System (ARES) model shown in figure 3. The ARES model has a streamlined fuselage shell that encloses the rotor controls and drive system. The fuselage shell, which is not usually installed when testing the ARES model in the HHF, was omitted during this test. The model rotor is powered by a variable-frequency, synchronous electric motor (rated at

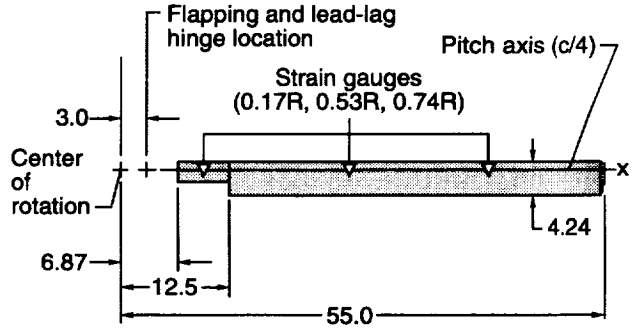

Figure 2. Rotor blade geometry. R is blade radius, and c is chord; all dimensions in inches.

47-hp output at 12000 rpm) that is connected to the rotor shaft through a belt-driven, two-stage, speed-reduction system. Collective pitch and cyclic pitch inputs are provided through a conventional swashplate arrangement. The swashplate is positioned by three electrically controlled hydraulic actuators, which are controlled remotely from the HHF control room. Signals from the blade strain gauge, as well as the signal from a strain-gauge-instrumented pitch link signal, are transferred from the rotating system to the fixed system through a 30-channel slip-ring assembly.

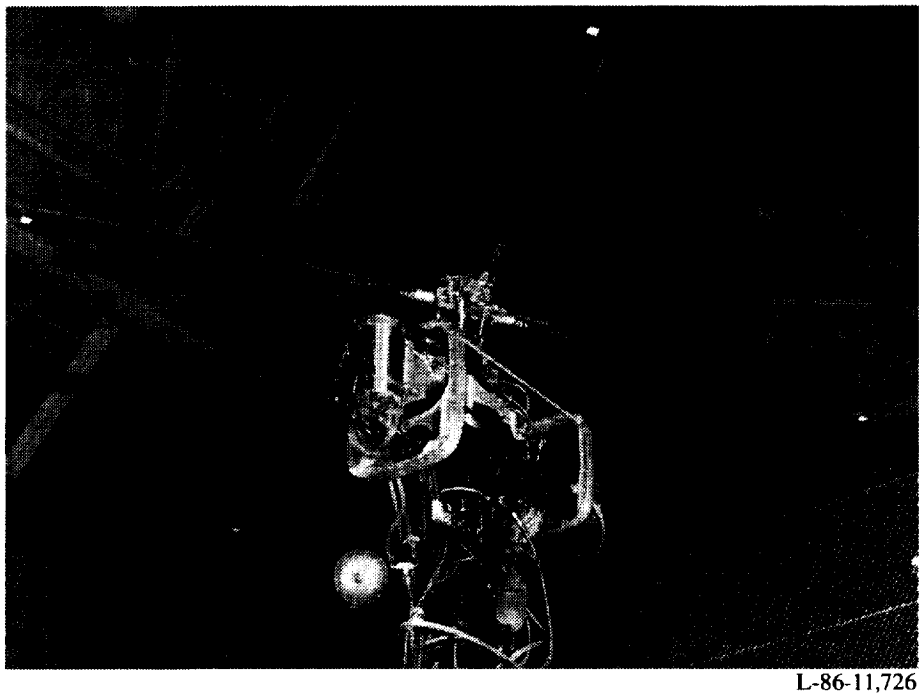

L-86-11,726

Figure 3. ARES model mounted in HHF.

Test Procedure

The experimental portion of this test was designed to provide accurate measurements of elastic blade mode frequencies over a range of rotor operating speeds. The experimental procedures described below are not necessarily the ideal techniques for experimentally measuring rotating blade frequencies, but are the best use of the existing ARES hardware and instrumentation for this purpose. For this experiment, only elastic blade modes with frequencies up to and including the first torsion mode were measured. Because of the limited blade instrumentation, no attempt was made to measure blade mode shapes during this test.

Rotating-frequency measurements for each mode were made at rotor speeds that ranged from 150 rpm to 660 rpm at approximately 100-rpm intervals. The nonoscillatory collective pitch of the blades was fixed at 0°. At each rpm increment, the blades were excited by sinusoidally oscillating the collective pitch of the rotor with the ARES hydraulic control system. This collective pitch oscillation frequency was varied over a 10- to 20-Hz frequency band in the vicinity of each modal frequency. The amplitude of vibratory loads caused by the movement of the swashplate together with the small amount of aerodynamic excitation present from the collective pitch oscillation was sufficient to excite all of the blade modes of interest.

Blade mode frequencies were determined by processing blade and pitch-link strain-gauge signals with an electronic signal analyzer. Output signals from the blade-mounted strain gauges were used as a measure of the blade modal deflection, while the pitch-link-mounted strain-gauge signal was used as a measure of the force input to the blade structure. From these two measurements, a frequency-response function could be generated using the signal analyzer. The frequency of the excited blade mode was then identified by looking for an amplitude peak in the frequency-response function.

Nonrotating modal frequencies were determined with a different procedure. For these measurements, the hub assembly, with a single attached blade, was removed from the ARES model and suspended so that the blade hung vertically. This method permitted measurements to be made without the blade resting on the hub flapping stops. A conventional impact-response test using a blade-mounted accelerometer, a signal analyzer, and an impact hammer was then performed. Nonrotating blade mode frequencies in this case were identified by looking for the amplitude peaks in the spectral-response function generated with the accelerometer signal.

NASTRAN Analysis

Blade Analytical Model

Analysis of the articulated rotor blade was performed using several versions of the MSC/NASTRAN finite-element-analysis computer code. The original,

pretest runs were performed using MSC/NASTRAN version 66b. Subsequent runs using version 67 and, more recently, version 68 were made to verify that procedures used with previous versions were still applicable and that the results had not changed.

The blade analytical model was constructed using standard finite-element-modeling techniques. A list of the complete input data deck is provided in appendix A. All material and structural property values for the blade model were taken from values shown in table 1. The blade structure was modeled entirely with CBEAM one-dimensional beam elements, with sectional masses and mass moments of inertia for all elements modeled as nonstructural mass.

The blade-root boundary conditions were approximated by allowing rotations only about the *Y*- and *Z*-axes of the global coordinate system, which represented motion about the flapping and lead-lag hinges. The blade-root lead-lag damper was modeled using a CELAS2 scalar spring element with an appropriate damping value and a small linear spring rate. Rotation about the *X*-axis (blade pitching degree of freedom) was constrained to be zero, representing in essence an infinitely stiff control system.

Rotating System Analysis Procedure

MSC/NASTRAN and COSMIC/NASTRAN have both been used to analyze the rotating modal behavior of compressor and turboprop blades (refs. 5 and 6). In these studies, plate, shell, and solid elements were used to model the blades. The computational procedure used in these studies required that two MSC/NASTRAN runs be made for each condition. First, a large-displacement analysis was made using MSC/NASTRAN solution 64. This solution sequence performs a large-displacement analysis on the rotating blade, computes steady-state displacements and stresses, and then stores the blade final stiffness and mass matrices of the blade model in a database. The frequencies and mode shapes were then computed with solution 63, using the saved matrices from the solution 64 run.

The current study also used a two-step process to obtain the blade frequencies and mode shapes although, as mentioned previously, beam elements are used here to model the rotor blade. At each desired rotor speed condition, the blade model was first analyzed using the nonlinear statics (database) MSC/NASTRAN solution sequence 66, which is the updated version of solution 64. This run calculated the deflections of the blade structure caused by a radial force field defined with the RFORCE card in the bulk data deck. Gravity forces and aerodynamic forces were neglected throughout this analysis, and only forces acting on the blade as a result of rotation were considered. The MSC/NASTRAN executive control cards, case control cards, and bulk data used for a sample solution 66 run are included in the listing in appendix A.

Once the static analysis of the blade had been completed, a modified normal modes analysis (solution 63) was performed as a "restart" job using the MSC/NASTRAN database files generated and saved from the solution 66 run. Two modifications were made in the solution 63 DMAP code to obtain the correct rotating-blade mode shapes and frequencies of the structure. The first modification was the inclusion of a standard MSC/NASTRAN rigid format DMAP alter (RF63D89) into the solution 63 source code. This DMAP alter allowed the stiffness matrix generated and saved from the solution 66 run, which included the differential stiffening effects of the radial forces acting on the rotor blade, to be used instead of the stiffness matrix normally generated in the solution 63 run. A second DMAP modification (NLGYRO.ALT) was made to include additional centrifugal softening terms in the stiffness matrix. NLGYRO.ALT also adds Coriolis terms to the damping matrix; however, for the normal modes analysis described here, damping and Coriolis terms can be ignored. This modified solution 63 DMAP source code, with the RF63D89 and NLGYRO.ALT DMAP alters included, was then recompiled and executed as a restart job using the previously generated solution 66 database files.

The nonrotating (0-rpm) case required no initial nonlinear statics run and was performed using the unmodified solution 63 normal-modes solution sequence.

The executive control cards and case control cards necessary to execute the solution 63 runs are shown in appendix B. Changes required between MSC/NASTRAN version 68 and earlier versions (66 and 67) are noted. The RF63D89 alter code, provided in the general distribution of MSC/NASTRAN, has not been shown here. The NLGYRO.ALT alter code, which was written originally for use with version 66b and is not usually provided in the general distribution, was obtained independently from MSC. Several modifications to this DMAP alter are necessary for it to be used with MSC/NASTRAN version 68. These modifications are noted in appendix C.

Presentation of Results

A comparison of the experimental and analytical frequency results is shown graphically in figure 4. This plot shows blade mode frequencies (Hz) versus rotor speed (rpm) for the first five elastic blade modes. The solid

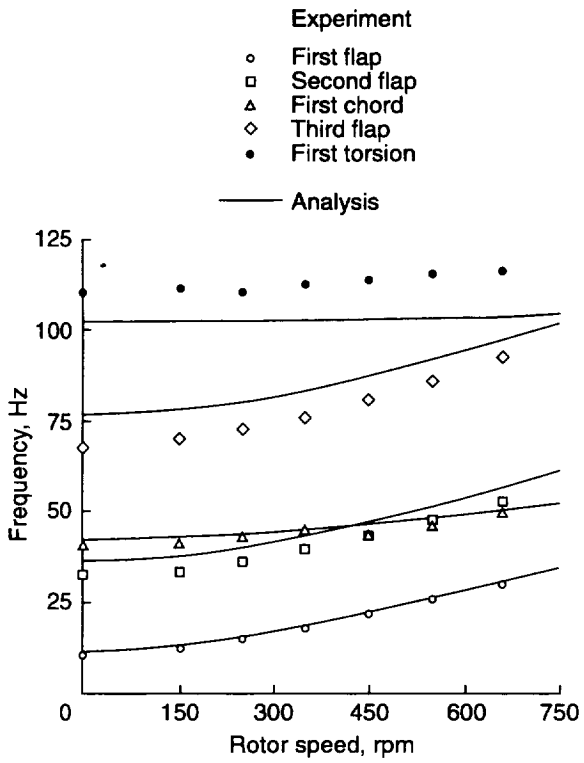

Figure 4. Comparison of experimental and analytical frequencies vs rotor speed. Rigid body flap and lead-lag modes not shown.

lines represent the analytical predictions of the blade mode frequencies made by MSC/NASTRAN. The symbols denote experimental frequency values measured in the HHF. A comparison of these experimental and analytical frequency values is also provided in table 2. Analytical calculations of the flapping and lead-lag rigid-body mode frequencies have been omitted. Repeatability in the frequency measurements was within ±1 Hz for the three flapping modes measured, and ±2 Hz for the chord-wise and torsion modes. Variations in the rotor rpm settings were very small, typically less than ±2 rpm.

Discussion of Results

The correlation of the MSC/NASTRAN-computed, rotating-blade frequencies with the experimentally measured frequencies was, overall, very good, with the best results being obtained for the lower flapping and chord-wise modal frequencies. With the exception of blade torsion, trends in mode frequency with rotor speed were adequately predicted by the analysis. The largest discrepancies between the analytical and experimental results occurred with the third elastic flap mode results and the first torsion mode results.

The discrepancies with the third flapping mode were thought to be due to inaccurate flapping stiffness data used in defining the analytical model. MSC/NASTRAN, when given accurate structural modeling information, generally does an excellent job of predicting the non-rotating modes and frequencies of a structure. As the nonrotating-frequency calculation for this mode was still significantly in error with the experimental value, the difference is thought to be due to the structural modeling of the blade and not a fundamental error with the MSC/NASTRAN procedures used in this study.

The discrepancies in the torsional frequency magnitude are thought to be due primarily to the "infinitely stiff" control system approximation used for the blade root boundary conditions. A finite stiffness associated with the pitching degree of freedom at the root would move the frequency magnitudes upward toward the experimentally measured values. The slight upward trend of the measured frequency with rotor speed was also not predicted in the analytical results. This trend is thought to be caused by the absence of a propeller-moment-type term in the NLGYRO.ALT alter code.

Table 2. Comparison of Experimental and Analytical Blade Frequencies

	Frequency, Hz at rotor speed of—													
	0 rpm		150 rpm		250 rpm		350 rpm		450 rpm		550 rpm		660 rpm	
Mode	Exper-iment	Analysis	Exper-iment	Analysis	Exper-iment	Analysis	Exper-iment	Analysis	Exper-iment	Analysis	Exper-iment	Analysis	Exper-iment	Analysis
1st flap	10.7	11.53	12.2	13.10	14.7	15.51	17.6	18.52	21.2	21.91	24.9	25.51	28.8	29.62
2nd flap	32.6	36.38	33.1	37.64	35.8	39.78	39.0	42.77	42.7	46.44	46.7	50.63	51.75	55.69
1st chord	41.0	42.44	41.1	42.82	42.8	43.49	44.4	44.48	43.0	45.75	45.2	47.30	49.1	49.29
3rd flap	67.8	76.80	70.0	77.97	72.5	80.01	75.3	82.95	80.4	86.70	85.3	91.11	91.5	96.52
1st torsion	110.3	102.05	111.0	102.06	110.0	102.09	112.0	102.12	113.0	102.18	114.5	102.28	115.0	102.53

Concluding Remarks

The rotating frequencies of a model articulated helicopter rotor blade were measured and compared to analytical frequency calculations performed using the MSC/NASTRAN finite-element structural analysis computer code. These results show that MSC/NASTRAN can, with slight modifications, adequately predict flapping and chordwise rotating modal characteristics of an articulated helicopter rotor blade structure. Accurate prediction of torsional frequencies and trends will most likely require some additional modifications to the MSC/NASTRAN DMAP source code.

NASA Langley Research Center
Hampton, VA 23681-0001
January 22, 1997

Appendix A

MSC/NASTRAN Solution 66 Input Data Deck

The material in this appendix constitutes the complete input data deck used to construct the blade analytical model.

```
$$$
```

```
$ GRID    ID      CP      X1      X2      X3      CD      PS      SEID
$-------2-------3-------4-------5-------6-------7-------8-------9-------A-------
GRID, 200,, 3.00, 0.0, 0.0,, 1234
GRID, 201,, 6.87, 0.0, 0.0
GRID, 202,, 8.87, 0.0, 0.0
GRID, 203,, 10.625, 0.0, 0.0
GRID, 204,, 3.00, 0.0, 0.0,, 123456
$
$-----------------------------------------------------------------------------
$ CONNECTIVITY:
$-----------------------------------------------------------------------------
$ BLADE CUFF AND ROOT (RS 3.0 TO 12.5)
$-----------------------------------------------------------------------------
$ CBEAM    EID     PID     GA      GB      X1      X2      X3
$-------2-------3-------4-------5-------6-------7-------8-------9-------A-------
CBEAM     200     200     200     201     0.0     1.0     0.0
CBEAM     201     201     201     202     0.0     1.0     0.0
CBEAM     202     202     202     203     0.0     1.0     0.0
CBEAM     203     203     203    1000     0.0     1.0     0.0
$
$ LEAD-LAG DAMPER ELEMENT
$-----------------------------------------------------------------------------
$ CELAS2   EID      K      G1      C1      G2      C2      GE      S
$-------2-------3-------4-------5-------6-------7-------8-------9-------A-------
CELAS2, 204, 464.0, 204, 6, 200, 6, 980.0
$
$-----------------------------------------------------------------------------
$ PROPERTY CARDS:
$-----------------------------------------------------------------------------
$-----------------------------------------------------------------------------
$ PBEAM    PID     MID      A       I1      I2     I12      J      NSM
$-------2-------3-------4-------5-------6-------7-------8-------9-------A-------
PBEAM, 200, 1000, 5.500, 0.5000, 0.5000, , 0.2632, 0.42511, +P2001
+P2001,,,,,,,,,+P2002
+P2002,,,,, 2.200-1
$
PBEAM, 201, 1000, 0.371, 0.1500, 0.0500, , 0.1316, 0.19380, +P2011
+P2011,,,,,,,,,+P2012
+P2012,,,,, 4.826-2
$
PBEAM, 202, 1000, 0.371, 0.0250, 0.0040, , 0.0105, 0.04086, +P2021
+P2021,,,,,,,,,+P2022
+P2022,,,,, 2.505-2
$
PBEAM, 203, 1000, 0.371, 0.0250, 0.0040, , 0.0105, 0.15113, +P2031
+P2031,,,,,,,,,+P2032
+P2032,,,,, 5.671-2
$
$
$$$$$$$$$$$$$$$$$$$$$$$$$$$$$$$$$$$$$$$$$$$$$$$$$$$$$$$$$$$$$$$$$$$$$$$$$$$
$$  FREON RESEARCH BLADE, LIGHTLY BALLASTED ( RS 12.5 TO 55.0 ) 4-9-92    $$
$$$$$$$$$$$$$$$$$$$$$$$$$$$$$$$$$$$$$$$$$$$$$$$$$$$$$$$$$$$$$$$$$$$$$$$$$$$
$
$-----------------------------------------------------------------------------
$ GEOMETRY:
$-----------------------------------------------------------------------------
$-----------------------------------------------------------------------------
$ GRID    ID      CP      X1      X2      X3      CD      PS      SEID
$-------2-------3-------4-------5-------6-------7-------8-------9-------A-------
GRID       1000          12.500   0.000   0.000
GRID       1001          13.000   0.000   0.000
GRID       1002          14.000   0.000   0.000
GRID       1003          15.000   0.000   0.000
GRID       1004          15.375   0.000   0.000
GRID       1005          15.600   0.000   0.000
GRID       1006          16.000   0.000   0.000
GRID       1007          17.000   0.000   0.000
GRID       1008          17.850   0.000   0.000
GRID       1009          18.000   0.000   0.000
GRID       1010          19.000   0.000   0.000
GRID       1011          20.000   0.000   0.000
GRID       1012          21.000   0.000   0.000
GRID       1013          22.000   0.000   0.000
```

```
GRID       1014          23.000   0.000   0.000
GRID       1015          23.750   0.000   0.000
GRID       1016          24.000   0.000   0.000
GRID       1017          25.000   0.000   0.000
GRID       1018          26.000   0.000   0.000
GRID       1019          27.000   0.000   0.000
GRID       1020          28.000   0.000   0.000
GRID       1021          28.250   0.000   0.000
GRID       1022          29.000   0.000   0.000
GRID       1023          29.150   0.000   0.000
GRID       1024          30.000   0.000   0.000
GRID       1025          31.000   0.000   0.000
GRID       1026          32.000   0.000   0.000
GRID       1027          33.000   0.000   0.000
GRID       1028          34.000   0.000   0.000
GRID       1029          35.000   0.000   0.000
GRID       1030          36.000   0.000   0.000
GRID       1031          37.000   0.000   0.000
GRID       1032          38.000   0.000   0.000
GRID       1033          39.000   0.000   0.000
GRID       1034          40.000   0.000   0.000
GRID       1035          41.000   0.000   0.000
GRID       1036          41.250   0.000   0.000
GRID       1037          42.000   0.000   0.000
GRID       1038          43.000   0.000   0.000
GRID       1039          44.000   0.000   0.000
GRID       1040          45.000   0.000   0.000
GRID       1041          46.000   0.000   0.000
GRID       1042          47.000   0.000   0.000
GRID       1043          48.000   0.000   0.000
GRID       1044          49.000   0.000   0.000
GRID       1045          50.000   0.000   0.000
GRID       1046          51.000   0.000   0.000
GRID       1047          52.750   0.000   0.000
GRID       1048          53.000   0.000   0.000
GRID       1049          54.000   0.000   0.000
GRID       1050          54.250   0.000   0.000
GRID       1051          55.000   0.000   0.000
$
$------------------------------------------------------------------------------
$ CONNECTIVITY:
$------------------------------------------------------------------------------
$------------------------------------------------------------------------------
$ CBEAM    EID     PID     GA      GB      X1      X2      X3
$-------2-------3-------4-------5-------6-------7-------8-------9-------A-------
CBEAM      1000    1000    1000    1001     0.0     1.0     0.0
CBEAM      1001    1001    1001    1002     0.0     1.0     0.0
CBEAM      1002    1001    1002    1003     0.0     1.0     0.0
CBEAM      1003    1001    1003    1004     0.0     1.0     0.0
CBEAM      1004    1004    1004    1005     0.0     1.0     0.0
CBEAM      1005    1004    1005    1006     0.0     1.0     0.0
CBEAM      1006    1004    1006    1007     0.0     1.0     0.0
CBEAM      1007    1004    1007    1008     0.0     1.0     0.0
CBEAM      1008    1008    1008    1009     0.0     1.0     0.0
CBEAM      1009    1008    1009    1010     0.0     1.0     0.0
CBEAM      1010    1008    1010    1011     0.0     1.0     0.0
CBEAM      1011    1008    1011    1012     0.0     1.0     0.0
CBEAM      1012    1008    1012    1013     0.0     1.0     0.0
CBEAM      1013    1008    1013    1014     0.0     1.0     0.0
CBEAM      1014    1008    1014    1015     0.0     1.0     0.0
CBEAM      1015    1015    1015    1016     0.0     1.0     0.0
CBEAM      1016    1015    1016    1017     0.0     1.0     0.0
CBEAM      1017    1015    1017    1018     0.0     1.0     0.0
CBEAM      1018    1015    1018    1019     0.0     1.0     0.0
CBEAM      1019    1015    1019    1020     0.0     1.0     0.0
CBEAM      1020    1015    1020    1021     0.0     1.0     0.0
CBEAM      1021    1021    1021    1022     0.0     1.0     0.0
CBEAM      1022    1021    1022    1023     0.0     1.0     0.0
CBEAM      1023    1021    1023    1024     0.0     1.0     0.0
CBEAM      1024    1021    1024    1025     0.0     1.0     0.0
CBEAM      1025    1021    1025    1026     0.0     1.0     0.0
CBEAM      1026    1021    1026    1027     0.0     1.0     0.0
CBEAM      1027    1021    1027    1028     0.0     1.0     0.0
```

```
CBEAM      1028    1021    1028    1029      0.0     1.0     0.0
CBEAM      1029    1021    1029    1030      0.0     1.0     0.0
CBEAM      1030    1021    1030    1031      0.0     1.0     0.0
CBEAM      1031    1021    1031    1032      0.0     1.0     0.0
CBEAM      1032    1021    1032    1033      0.0     1.0     0.0
CBEAM      1033    1021    1033    1034      0.0     1.0     0.0
CBEAM      1034    1021    1034    1035      0.0     1.0     0.0
CBEAM      1035    1021    1035    1036      0.0     1.0     0.0
CBEAM      1036    1021    1036    1037      0.0     1.0     0.0
CBEAM      1037    1021    1037    1038      0.0     1.0     0.0
CBEAM      1038    1021    1038    1039      0.0     1.0     0.0
CBEAM      1039    1021    1039    1040      0.0     1.0     0.0
CBEAM      1040    1021    1040    1041      0.0     1.0     0.0
CBEAM      1041    1021    1041    1042      0.0     1.0     0.0
CBEAM      1042    1021    1042    1043      0.0     1.0     0.0
CBEAM      1043    1021    1043    1044      0.0     1.0     0.0
CBEAM      1044    1021    1044    1045      0.0     1.0     0.0
CBEAM      1045    1021    1045    1046      0.0     1.0     0.0
CBEAM      1046    1046    1046    1047      0.0     1.0     0.0
CBEAM      1047    1047    1047    1048      0.0     1.0     0.0
CBEAM      1048    1048    1048    1049      0.0     1.0     0.0
CBEAM      1049    1049    1049    1050      0.0     1.0     0.0
CBEAM      1050    1050    1050    1051      0.0     1.0     0.0
$
$-------------------------------------------------------------------------------
$ PROPERTY CARDS:
$-------------------------------------------------------------------------------
$-------------------------------------------------------------------------------
$ PBEAM    PID     MID       A       I1      I2      I12      J       NSM
$-------2-------3-------4-------5-------6-------7-------8-------9-------A-------
PBEAM,1000,1000,0.377,0.03550,0.00394,,0.03940,0.14048,+P001
+P001,,,,,,,,,+P002
+P002,,,,, 5.559-2,,,,+P003
+P003, 0.00, 0.0, 0.00, 0.0
$
PBEAM,1001,1000,0.386,0.02520,0.00249,,0.00976,0.3134-1,+P011
+P011,,,,,,,,,+P012
+P012,,,,, 2.779-2,,,,+P013
+P013, 0.00, 0.0, 0.00, 0.0
$
PBEAM,1004,1000,0.339,0.02520,0.00249,,0.00976,0.4376-1,+P041
+P041,,,,,,,,,+P042
+P042,,,,, 2.961-2,,,,+P043
+P043, 0.00, 0.0, 0.00, 0.0
$
PBEAM,1008,1000,0.278,0.03040,0.00231,,0.00674,0.4123-1,+P081
+P081,,,,,,,,,+P082
+P082,,,,, 2.888-2,,,,+P083
+P083, 0.00, 0.0, 0.00, 0.0
$
PBEAM,1015,1000,0.249,0.02636,0.00181,,0.00565,0.400-1,+P151
+P151,,,,,,,,,+P152
+P152,,,,, 2.810-2,,,,+P153
+P153, 0.00, 0.0, 0.00, 0.0
$
PBEAM,1021,1000,0.224,0.02447,0.00151,,0.00485,0.3903-1,+P211
+P211,,,,,,,,,+P212
+P212,,,,, 2.756-2,,,,+P213
+P213, 0.00, 0.0, 0.00, 0.0
$
PBEAM,1046,1000,0.247,0.02447,0.00151,,0.00485,0.3903-1,+P461
+P461,,,,,,,,,+P462
+P462,,,,, 2.756-2,,,,+P463
+P463, 0.00, 0.0, 0.00, 0.0
$
PBEAM,1047,1000,0.279,0.02448,0.00160,,0.00502,0.4125-1,+P471
+P471,,,,,,,,,+P472
+P472,,,,, 2.826-2,,,,+P473
+P473, 0.00, 0.0, 0.00, 0.0
$
PBEAM,1048,1000,0.305,0.05000,0.00500,,0.01435,0.7867-1,+P481
+P481,,,,,,,,,+P482
+P482,,,,, 3.984-2,,,,+P483
```

```
+P483, -0.106, 0.0, -0.106, 0.0
$
PBEAM,1049,1000,0.099,0.04000,0.00400,,0.01148,0.607-1,+P491
+P491,,,,,,,,,+P492
+P492,,,,, 3.563-2,,,,+P493
+P493, -0.17, 0.0, -0.17, 0.0
$
PBEAM,1050,1000,0.05,0.00500,0.00050,,0.01435,0.1101-1,+P501
+P501,,,,,,,,,+P502
+P502,,,,, 4.401-3,,,,+P503
+P503, -0.940, 0.0, -0.940, 0.0
$
$-------------------------------------------------------------------------------
$ MATERIAL PROPERTY CARDS:
$-------------------------------------------------------------------------------
$ 1000: FIBERGLASS BLADE (ASSUMED PROPERTIES)
$-------------------------------------------------------------------------------
$          MID      E       G       NU      RHO
$-------2-------3-------4-------5-------6-------7-------8-------9-------A-------
MAT1       1000   1.0+7            0.3
$
$
ENDDATA
```

Appendix B

MSC/NASTRAN Solution 63 Restart Data Deck

This appendix presents the executive control cards and the case control cards required to execute the solution 63 runs.

```
RESTART
```

(use this executive control section for MSC/NASTRAN version 66 or 67:)

```
$
$$$
```

```
LABEL=(CF LOAD 11 HZ ROTATION)
SUBTITLE= NORMAL MODES RESTART SOL 63
$
ECHO=BOTH
DISPLACEMENT=ALL
OLOAD=ALL
$
SEALL=ALL
$
LOAD=1
$
METHOD=10
$
BEGIN BULK
$
$
$$$
```

Appendix C

Modifications to NLGYRO.ALT for Use With MSC/NASTRAN Version 68

Much of the DMAP language was changed between MSC/NASTRAN Version 68 and earlier versions. Because of this change, two minor changes in the original version 66b NLGYRO.ALT DMAP source code (obtained from MSC) are required for it to execute properly under MSC/NASTRAN version 68. These modifications follow.

1. In line 1 (ignoring comments), change

```
ALTER 492 $
```

to

```
ALTER 504 $
```

2. In line 23, change

```
VECPLOT    ,,BGPDT,EQEXIN,CSTM,,/RBGLOBAL///4/ $
```

to

```
VECPLOT    ,,BGPDT,EQEXIN,CSTM,,,,/RBGLOBAL///4/ $
```

(i.e., add two commas after CSTM.)

References

1. Anon.: *MSC/NASTRAN User's Manual—MSC/NASTRAN Version 66*. MacNeal-Schwendler Corp., 1988.

2. Joseph, Jerrard A., ed.: *MSC/NASTRAN Application Manual—MSC/NASTRAN Version 66A*. MacNeal-Schwendler Corp., 1991.

3. Mack, Wayne V., ed.: *MSC/DYNA Theoretical Manual—MSC/DYNA Version 1*. MacNeal-Schwendler Corp., 1989.

4. Lee, Sang H., ed.: *Preliminary MSC/NASTRAN Handbook for Nonlinear Analysis*. MacNeal-Schwendler Corp., 1991.

5. Lawrence, Charles; Aiello, Robert A.; Ernst, Michael A.; and McGee, Oliver G.: *A NASTRAN Primer for the Analysis of Rotating Flexible Blades*. NASA TM-89861, 1987.

6. McGee, Oliver G.: *Finite Element Analysis of Flexible, Rotating Blades*. NASA TM-89906, 1987.

REPORT DOCUMENTATION PAGE

Form Approved
OMB No. 0704-0188

Public reporting burden for this collection of information is estimated to average 1 hour per response, including the time for reviewing instructions, searching existing data sources, gathering and maintaining the data needed, and completing and reviewing the collection of information. Send comments regarding this burden estimate or any other aspect of this collection of information, including suggestions for reducing this burden, to Washington Headquarters Services, Directorate for Information Operations and Reports, 1215 Jefferson Davis Highway, Suite 1204, Arlington, VA 22202-4302, and to the Office of Management and Budget, Paperwork Reduction Project (0704-0188), Washington, DC 20503.

1. AGENCY USE ONLY *(Leave blank)*	2. REPORT DATE	3. REPORT TYPE AND DATES COVERED
	June 1997	Technical Memorandum

4. TITLE AND SUBTITLE
Rotating Shake Test and Modal Analysis of a Model Helicopter Rotor Blade

5. FUNDING NUMBERS
WU 505-63-36-02

A5008

6. AUTHOR(S)
W. Keats Wilkie, Paul H. Mirick, and Chester W. Langston

7. PERFORMING ORGANIZATION NAME(S) AND ADDRESS(ES)
NASA Langley Research Center
Hampton, VA 23681-0001

Vehicle Technology Center
U.S. Army Research Laboratory
NASA Langley Research Center
Hampton, VA 23681-0001

8. PERFORMING ORGANIZATION REPORT NUMBER
L-17352

9. SPONSORING/MONITORING AGENCY NAME(S) AND ADDRESS(ES)
National Aeronautics and Space Administration
Washington, DC 20546-0001
and
U.S. Army Research Laboratory
Adelphi, MD 20783-1145

10. SPONSORING/MONITORING AGENCY REPORT NUMBER
NASA TM-4760

ARL-TR-1389

11. SUPPLEMENTARY NOTES
Wilkie, Mirick, and Langston: Vehicle Technology Center, ARL, Langley Research Center, Hampton, VA.

12a. DISTRIBUTION/AVAILABILITY STATEMENT
Unclassified–Unlimited
Subject Category 05
Availability: NASA CASI (301) 621-0390

12b. DISTRIBUTION CODE

13. ABSTRACT *(Maximum 200 words)*
Rotating blade frequencies for a model generic helicopter rotor blade mounted on an articulated hub were experimentally determined. Testing was conducted using the Aeroelastic Rotor Experimental System (ARES) testbed in the Helicopter Hover Facility (HHF) at Langley Research Center. The measured data were compared to pretest analytical predictions of the rotating blade frequencies made using the MSC/NASTRAN finite-element computer code. The MSC/NASTRAN solution sequences used to analyze the model were modified to account for differential stiffening effects caused by the centrifugal force acting on the blade and rotating system dynamic effects. The correlation of the MSC/NASTRAN-derived frequencies with the experimental data is, in general, very good although discrepancies in the blade torsional frequency trends and magnitudes were observed. The procedures necessary to perform a rotating system modal analysis of a helicopter rotor blade with MSC/NASTRAN are outlined, and complete sample data deck listings are provided.

14. SUBJECT TERMS
Helicopters; Model rotor testing; Rotor analysis; NASTRAN; Structural dynamics

15. NUMBER OF PAGES
16

16. PRICE CODE
A03

17. SECURITY CLASSIFICATION OF REPORT	18. SECURITY CLASSIFICATION OF THIS PAGE	19. SECURITY CLASSIFICATION OF ABSTRACT	20. LIMITATION OF ABSTRACT
Unclassified	Unclassified	Unclassified	